Significant motions of a multi-purpose floating offshore structure due to environmental conditions

Thomas P. Mazarakos, Dimitrios N. Konispoliatis, Takvor H. Soukisian, and Spyridon A. Mavrakos

Abstract—**This paper presents a coupled hydro-aero-elastic analysis method for the evaluation of loads on a multi-purpose floating structure, suitable for offshore wind and wave energy sources exploitation. The analysis method incorporates properly, the solutions of the diffraction, the pressure- and the motion- dependent radiation problems around the floating structure along with the aerodynamics of the Wind Turbine (WT). The floating structure, which is exposed to the action of regular and irregular waves in finite depth waters, encompasses an array of three hydrodynamically interacting Oscillating Water Column (OWC) devices consisting of concentric vertical cylinders, moored through tensioned tethers as a Tension Leg Platform (TLP) supporting a 10 MW WT. The wave loads on the floater are approximated using matched axisymmetric eigenfunction expansions. The objective of the analysis is to investigate which sea states yield the significant motions of the offshore structure due to operating wave conditions obtained through wave hindcast time series, in the Mediterranean Sea near to Sicily Island.**

Keywords—**Environmental conditions, mooring system, multi-purpose structure, oscillating water column, wind turbine.**

Paper ID: 52/1504/DV/87. Track: Wave Hydrodynamic Modelling.

The research has been financed by the project FHMES: Floating Hybrid Mooring Wind Turbine Energy System. This project has received funding from the Hellenic Foundation for Research and Innovation (HFRI) and the General Secretariat for Research and Technology (GSRT), under grant agreement No 720 [61/5047].

T.P. Mazarakos is with the Laboratory for Floating Structures and Mooring Systems, School of Naval Architecture and Marine Engineering, National Technical University of Athens, 9 Heroon Polytechniou Avenue, GR 15773, Greece (e-mail: tmazarakos@naval.ntua.gr).

D.N. Konispoliatis is with the Laboratory for Floating Structures and Mooring Systems, School of Naval Architecture and Marine Engineering, National Technical University of Athens, 9 Heroon Polytechniou Avenue, GR 15773, Greece (e-mail: dkonisp@naval.ntua.gr).

T.H. Soukissian is with Hellenic Center for Marine Research, 46.7km Athens Sounio Avenue, GR 19013, Greece (e-mail: tsouki@hcmr.gr).

S.A. Mavrakos is with the Laboratory for Floating Structures and Mooring Systems, School of Naval Architecture and Marine Engineering, National Technical University of Athens, 9 Heroon Polytechniou Avenue, GR 15773, Greece (e-mail: mavrakos@naval.ntua.gr) and with the Hellenic Center for Marine Research, 46.7km Athens Sounio Avenue, GR 19013, Greece (e-mail: mavrakos@hcmr.gr).

I. Introduction

OFFSHORE wind energy is currently attracting most of the research attention within the sector. In the present paper, a multi-cylinder TLP design concept conceived as supporting structure of the DTU 10MW WT [1] is analysed.

As far as the case of multiple wave energy converters (WEC) is concerned, OWC devices consisted of circular or concentric cylindrical chambers have been mainly investigated. Theoretical studies in the context of freely floating WEC's have been developed in regular ([2], [3]) and irregular wave fields [4]. In the present contribution, each examined OWC device consists of an exterior partially immersed toroidal oscillating chamber of finite volume supplemented by a concentric interior piston- like truncated cylinder in which the tension tether is attached.

The main difference between an isolated OWC device and an array of such devices is the hydrodynamic interaction phenomena between the array's members. Each device of the configuration scatters waves towards the others, which in turn scatter waves contributing to the excitation of the initial device and so on. Thus, the total wave field around each body of the multi-body configuration is obtained by superposing the incident wave potential and various orders of successively reflected waves emanating from all the devices of the arrangement using the physical idea of multiple scattering ([5], [6], [7]).

Another challenge that has presented in the last years is the design of multipurpose floating structures that absorbs not only wind ([8], [9]) but also wave energy. Lately, many attempts have been conducted related to the hydrodynamic analysis and the optimization of those structures, studying different arrays and characteristics of the configuration. In ([10], [11], [12]) the coupled hydro-aero-elastic analysis of a multipurpose floating structure, under the action of regular surface waves is examined. The numerical results were dealt with the motions and the mean second order loads of the floating structure.

Furthermore, in [13] a parametric hydrodynamic analysis was made that compared the analytical results of

a triangular, quadrate and pentagonal floater with three, four and five identical OWC devices respectively.

II. FLOATING SYSTEM

The examined floating system has been defined for the DTU 10MW WT [1]. The tower of the WT is cantilevered at an elevation of 10m above the sea water level (SWL) to the top of the main column of the floating platform. In the present contribution the examined three identical OWC devices, consisting of concentric vertical cylinders, are placed at the corners of a triangular floater, oscillating about their mean equilibrium position moving as a unit (Figures 1-2).

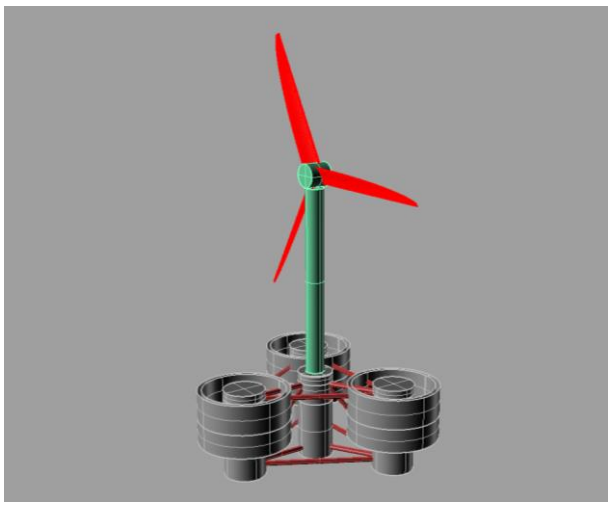

Fig. 1. 3-D representation of the floating platform.

A regular monochromatic wave train is propagating along the positive x-axis (Figure 2) causing the captured water column to oscillate in the annular chamber, compressing and decompressing the air above the inner water surface. As a result, there is an air flow moving forwards and backwards through a turbine placed at the top of each device's chamber coupled to an electric generator. The flow rate through each turbine can be prevented from becoming excessive in extreme wave conditions by equipping each device with air valves. In the centre of the platform a solid cylindrical body is arranged in order to support the WT (Figures 1-2).

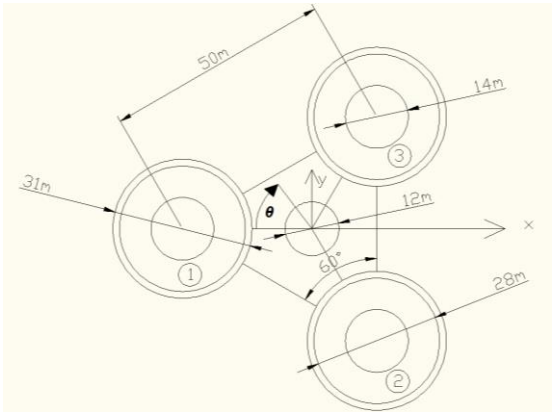

Fig. 2. Top view of the floating platform.

A summary of the geometry, including the diameters of each of the structural members is given in Table I. These properties are all relative to the undisplaced position of the platform.

TABLE I
FLOATING PLATFORM GEOMETRY

Depth of platform base below SWL (total draught)	20.00 m
Elevation of main column (tower base) above SWL	10.00 m
Elevation of offset columns above SWL	10.00 m
Spacing between columns	50.00 m
Draught of the structure	20.00 m
Radius of main column	6.00 m
Radius of inner concentric cylindrical body	7.00 m
Oscillating chamber thickness of each device	1.50 m
Outer radius of the Oscillating chamber on each device	15.50 m
Oscillating chamber's draught	8.00 m
Radius of pontoons and cross braces	0.80 m

The mass, including ballast, of the floating platform is 9550 t. This mass is calculated such that the combined weight of the rotor-nacelle assembly, tower, structural mass of the platform and the pretension of the tendons, plus the weight of the mooring system in water, balances with the buoyancy (i.e. weight of the displaced fluid) of the platform in the static equilibrium position in still water. The centre of mass (CM) of the floating platform, including ballast, is located at 11.182 m along the platform centre-line below the SWL. The roll and pitch inertias of the floating platform about its CM are 9.78E6 tm^2 and 9.78E6 tm^2 with respect to the platform x-axis and y-axis respectively, while the yaw inertia of the floating platform about its centerline is 11.70E6 tm^2.

In the corresponding frequency domain formulation, the contribution of the WT is projected on the 6 floater rigid body motions. By linearizing all terms with respect to the case of zero floater motions (static equilibrium), the added mass, the damping and the stiffness matrices are defined which contribute the WT's aerodynamic, inertial-gyroscopic and gravitational effect on the floater [14]. The height of the selected WT's tower is 105.63 m, the CM of the WT is 46.7 m and the mass of the WT is 1200 t. The roll and pitch inertias of the latter about its CM are 1.089E7 tm^2 and 1.089E7 tm^2 respectively, while the yaw inertia about its centre line is 9.757E4 tm^2.

To secure the platform, the floating structure is moored with a TLP mooring system of three tendon pipes each spread symmetrically about the platform z-axis.

The mooring forces $f_{i,mooring}$ acting on the platform in the i-th direction can be derived by:

$$F_{i,mooring} = C_{i,j\ mooring}\xi_{j0}\ , \qquad j = 1, \dots 6 \qquad (1)$$

Here, ξ_{j0} is the motion displacement of the entire system at the j-th direction with respect to the global co-ordinate system G.

The mooring lines stiffness matrix, $C_{ij,mooring}$ is a (6x6) square matrix the elements of which, are obtained:

$$C_{1,1} = C_{2,2} = \sum_{n=1}^{3} \frac{T_n}{L}, \quad C_{3,3} = \frac{EA}{L} \tag{2}$$

Here, T_n are the tendon pretension forces; E is the Young's modulus of elasticity; A is the total cross-section area and L is the tendon's length.

The fairleads (body fixed locations where the mooring tendons are mounted to the platform) are located at the base of the offset columns, at a depth of 20.0 m below the SWL. The anchors (fixed to the inertia frame) are located at a water depth of 200 m below the SWL. Each of the 3 tendons pipe configuration has an unstretched length of 180 m, a diameter of 1.22 m, an equivalent mass per unit length of 1.22 t/m, an equivalent submerged weight per unit length of 10.5 kN/m. The thickness of each tendon pipe is 0.0422 m. The pretension of each tendon is 18840 kN. The mooring line stiffness kxx of each tendon is 104.68 kN/m and the mooring line stiffness kzz of each tendon is 173334 kN/m.

III. Formulation of the Hydrodynamic Problem

Hydrodynamic loads on the structure include contributions from linear hydrostatics, the diffraction problem (linear excitation from the incident waves) and the linear motion - (due to the body motions) and pressure - dependent (due to the OWC's devices) radiation problems.

The analytical calculations are obtained using the in-house developed computer code HAMVAB (Hydrodynamic Analysis of Multiple Vertical Axisymmetric Bodies, [15]) software in FORTRAN programming language that is properly extended to account for the pressure - dependent radiation problems due to the pressure head developed in the OWC's air chamber [2].

The investigation of the dynamic equilibrium of the forces acting on the freely floating array of OWC devices/body without the WT leads to the following well-known system of differential equations of motions, in the frequency domain, i.e.:

$$\sum_{j=1}^{6} \left[-\omega^2 \left(M_{i,j} + A_{i,j} + \frac{i}{\omega} B_{i,j} \right) + C_{i,j} \right] \xi_{j0} = F_{P,i} + F_i \tag{3}$$

for i=1,…,6.

Where $M_{i,j}$ and $C_{i,j}$ are elements of the (6x6) mass and hydrostatic stiffness matrices of the entire configuration; $A_{i,j}$ and $B_{i,j}$ are the hydrodynamic masses and potential damping of the entire configuration; F_i are the exciting forces acting on the multi-body system at the i-th direction; $F_{P,i}$ are the pressure hydrodynamic forces acting on the multi-body system at the i–th direction; ξ_{j0} is the motion displacement of the entire structure as presented in Eq. (1).

By inserting the TLP mooring system and the WT characteristics in the multi- body system, Eq. (3) can be reduced to the following form ([10], [14]), describing the couple hydro-aero-elastic problem of the investigated moored multi-purpose floating structure in the frequency domain:

$$\sum_{j=1}^{6} \left[-\omega^2 \left(M_{i,j} + A_{i,j} + M_{i,j}^{WT} + \frac{i}{\omega} B_{i,j} + \frac{i}{\omega} B_{i,j}^{WT} \right) + C_{i,j} + C_{i,j}^{WT} + C_{mooring} \right] \xi_{j0} = F_{P,i} + F_i \tag{4}$$

where $M_{i,j}^{WT}$, $B_{i,j}^{WT}$ and $C_{i,j}^{WT}$, are the mass, damping and stiffness matrices originating from the WT aerodynamic, inertial-gyroscopic and gravitational loading respectively, while $C_{mooring}$ is the mooring lines stiffness matrix.

The non-dimensional amplitudes of the first order body motions have been plotted for various directions against the incoming wave frequency ω (Response Amplitude Operators - RAO's). The wave incidence directions have been chosen for each 30 degrees, thus the angle of wave impact θ is in the range of 0 to 60 degrees (see Fig. 2).

The frequency dependent motions ξ_{j0} of a floating structure in the j-th direction (j = 1, 2, …, 6), can be expressed as:

$$\xi_j(t) = Re\left\{ |\xi_{j0}| e^{-i(\omega t - \varphi_j)} \right\} \tag{5}$$

Where $|\xi_{j0}|$ and φ_j are the modulus and the phase of the complex amplitude of motion ξ_j, respectively and ω is the frequency of the wave excitation. The modulus of body's motions is given in the following graphs in non-dimensional form.

The translational modes of motions are made dimensionless using the following formula:

$$s_{j0} = \frac{|\xi_{j0}|}{H/2}, \quad [\mathrm{m/m}] \tag{6}$$

where j=1, 2, 3 (i.e. surge, sway and heave), and $H/2$ the incident wave amplitude (m).

For the sake of completeness, some representative results concerning the surge motion RAOs, are included here (Figure 3).

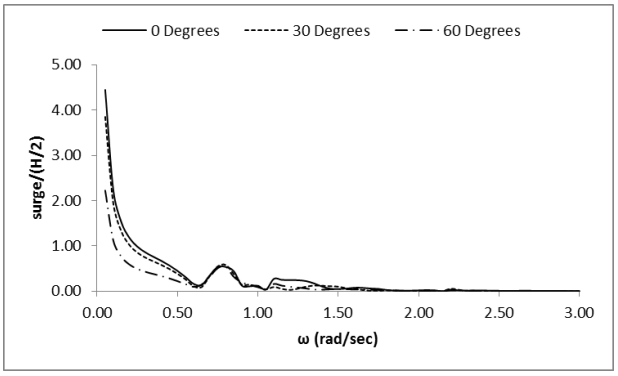

Fig. 3. Non-dimensional RAO's of surge motion, for various wave angles, versus wave frequency ω.

IV. ENVIRONMENTAL CONDITIONS

The wave climate in the southern part of Sicily Island with coordinates ~37.30° N, ~12.69° E; at water depth around 200m (Figure 4) for wave energy assessment purposes (as e.g., to identify the overall most energetic sea state in the area) can be described through the following *Tp-Hs* frequency Table II. The wave data have been obtained by the ERA-20C data set, published by the European Centre For Medium-Range Weather Forecasts (ECMWF), [16]. Let us note that ERA5 data set was not available during the project FHMES. The obtained values refer to the total available sample for the period 1980-2010, while the N-years design values of significant wave height, spectral peak period and wind speed have been also estimated, for N=10-100 years ([17], [18[, [19]). The cell with the largest frequency of occurrence is shown with boldface digits.

Fig. 4. The examined location in the Mediterranean Sea (from Google Earth)

In the design process of mooring systems, specific requirements are imposed related to the safety and functionality of the anchored structure ([20]). Based on the API's regulations, in the case of an anchored construction, the underlying condition is that the maximum displacement of the top of the line receiving the external load in the direction of its length, should not be greater than 5% of the water depth. This percentage becomes 10% in the case of extreme sea conditions.

TABLE II
BIVARIATE FREQUENCY TABLE FOR LOCATION 37.30° N, 12.69° E (SOUTH WESTERN PART OF SICILY ISLAND)

Tp (s)	*Hs* (m)						
	0 – 1	1 – 2	2 – 3	3 – 4	4 – 5	5 – 6	6 – 7
2 – 3	0.014	0.000	0.000	0.000	0.000	0.000	0.000
3 – 4	0.180	0.000	0.000	0.000	0.000	0.000	0.000
4 – 5	**0.240**	0.022	0.000	0.000	0.000	0.000	0.000
5 – 6	0.150	0.076	0.001	0.000	0.000	0.000	0.000
6 – 7	0.084	0.082	0.016	0.000	0.000	0.000	0.000
7 – 8	0.017	0.037	0.026	0.003	0.000	0.000	0.000
8 – 9	0.006	0.012	0.012	0.007	0.001	0.000	0.000
9 – 10	0.001	0.002	0.003	0.004	0.002	0.000	0.000
10 – 11	0.000	0.000	0.000	0.000	0.001	0.000	0.000
11 – 12	0.000	0.000	0.000	0.000	0.000	0.000	0.000

Having calculated the RAO's of the first-order surge motions of the floating structure due to the presence of simple harmonic waves for various angles of incidence (see Section III); the motion response spectra is obtained herein by multiplying the wave spectrum with the RAO squared and integrating over the wave directions, i.e.:

$$S_i(\omega) = (RAO)^2 S_\zeta(\omega) \tag{7}$$

where i indicates the degree of freedom (here i=1: surge), S_i is the response spectrum and S_ζ is the wave spectrum.

The significant values of the response spectrum are:

$$x_{1/3} = 2\sqrt{\int_0^\infty S_i(\omega)d\omega} \tag{8}$$

In Tables III, IV and V the significant values for the surge motions (in m) of the structure for the operating conditions, for wave heading angles 0, 30 and 60 degrees, are presented respectively, by applying the Jonswap spectrum ([4], [21], [22]). The cell with the largest value of surge motion is shown with boldface digits. In all cases the surge motions of the system does not exceed the API's limits.

TABLE III
SIGNIFICANT SURGE MOTIONS TABLE FOR LOCATION 37.30° N, 12.69° E (SOUTH WESTERN PART OF SICILY ISLAND) (0 DEGREES)

Tp (s)	*Hs* (m)						
	0 – 1	1 – 2	2 – 3	3 – 4	4 – 5	5 – 6	6 – 7
2 – 3	0.005	0	0	0	0	0	0
3 – 4	0.006	0.019	0	0	0	0	0
4 – 5	0.025	0.076	0	0	0	0	0
5 – 6	0.040	0.119	0.198	0	0	0	0
6 – 7	0.039	0.117	0.194	0	0	0	0
7 – 8	0.058	0.174	0.289	0.405	0.521	0	0
8 – 9	0.085	0.255	0.425	0.596	0.766	0.936	0
9 – 10	0.113	0.338	0.564	0.789	1.014	1.240	0
10 – 11	0.142	0.426	0.710	0.994	1.277	1.561	1.845
11 – 12	0	0	0	1.130	0	1.776	**2.099**

TABLE IV
SIGNIFICANT SURGE MOTIONS TABLE FOR LOCATION 37.30° N, 12.69° E (SOUTH WESTERN PART OF SICILY ISLAND) (30 DEGREES)

Tp (s)	*Hs* (m)						
	0 – 1	1 – 2	2 – 3	3 – 4	4 – 5	5 – 6	6 – 7
2 – 3	0.000	0	0	0	0	0	0
3 – 4	0.005	0.015	0	0	0	0	0
4 – 5	0.017	0.052	0	0	0	0	0
5 – 6	0.023	0.069	0.116	0	0	0	0
6 – 7	0.046	0.137	0.228	0	0	0	0
7 – 8	0.083	0.248	0.413	0.578	0.743	0	0
8 – 9	0.092	0.276	0.460	0.643	0.827	1.011	0
9 – 10	0.074	0.222	0.371	0.519	0.667	0.815	0
10 – 11	0.068	0.205	0.341	0.478	0.614	0.751	0.887
11 – 12	0	0	0	0.544	0	0.855	1.010

TABLE V
SIGNIFICANT SURGE MOTIONS TABLE FOR LOCATION 37.30° N, 12.69° E (SOUTH WESTERN PART OF SICILY ISLAND) (60 DEGREES)

Tp (s)	*Hs* (m)						
	0 – 1	1 – 2	2 – 3	3 – 4	4 – 5	5 – 6	6 – 7
2 – 3	0.000	0	0	0	0	0	0
3 – 4	0.002	0.007	0	0	0	0	0
4 – 5	0.011	0.034	0	0	0	0	0
5 – 6	0.027	0.082	0.137	0	0	0	0
6 – 7	0.045	0.135	0.225	0	0	0	0
7 – 8	0.078	0.233	0.388	0.544	0.699	0	0
8 – 9	0.086	0.259	0.431	0.603	0.776	0.948	0
9 – 10	0.069	0.208	0.346	0.484	0.623	0.761	0
10 – 11	0.059	0.176	0.293	0.410	0.527	0.645	0.762
11 – 12	0	0	0	0.408	0	0.641	0.758

The analysis methodology presented in the previous sections, has been applied to the case of REFOS [23] platform. More specifically, in Figures 5, 7 and 9, the significant surge motion (m) contour map of the REFOS platform for each wave condition in the installation location (0, 30 and 60 degrees respectively) is depicted.

In Figures 6, 8, 10, the 3-D significant surge motion (m) surface of the REFOS platform for each wave condition in the installation location (0, 30 and 60 degrees respectively) can be seen.

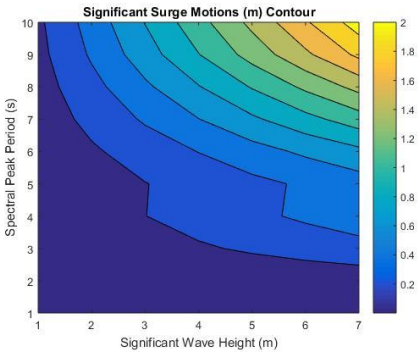

Fig. 5 Significant surge motion (m) contour of the REFOS platform for each wave condition in the installation location for wave heading angle 0 degrees

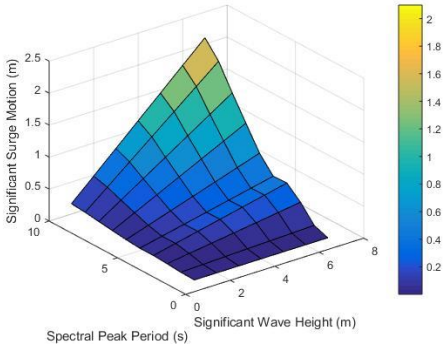

Fig. 6. 3-D Significant surge motion (m) surface of the REFOS platform for each wave condition in the installation location for wave heading angle 0 degrees

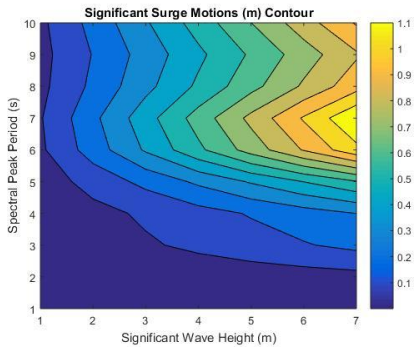

Fig. 7 Significant surge motion (m) contour of the REFOS platform for each wave condition in the installation location for wave heading angle 30 degrees

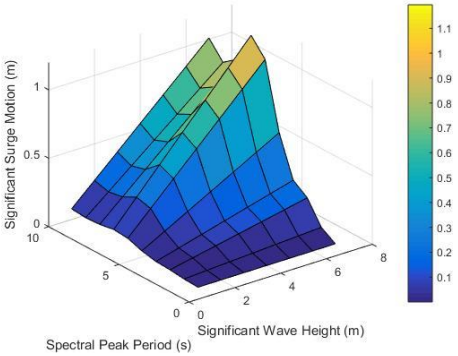

Fig. 8. 3-D Significant surge motion (m) surface of the REFOS platform for each wave condition in the installation location for wave heading angle 30 degrees

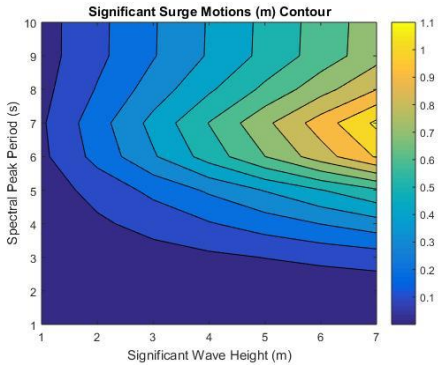

Fig. 9 Significant surge motion (m) contour of the REFOS platform for each wave condition in the installation location for wave heading angle 60 degrees

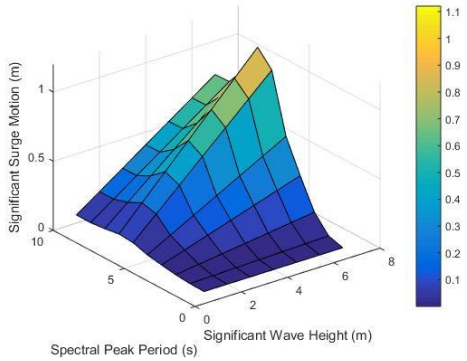

Fig. 10. 3-D Significant surge motion (m) surface of the REFOS platform for each wave condition in the installation location for wave heading angle 60 degrees

V. CONCLUSION

A TLP floater for the DTU 10MW WT has been presented encompassing three cylinders, which include three OWC devices.

For this design, RAOs of the complete system have been calculated using a frequency domain solution, considering the WTs contribution on the floater's degrees of freedom after a linearization process based on a Reduced Order Model (ROM) model.

It can be seen that the cells with the maximum significant surge motion are:
Table III: (6-7m; 11-12s), for wave heading 0 degrees
Table IV: (6-7m; 11-12s), for wave heading 30 degrees
Table V: (5-6m; 8-9s) for wave heading 60 degrees.

The tethers provide sufficient restoring in surge to adequately limit the steady - state offset in surge.

Due to API Recommended Practice, the significant surge motion of the TLP floater does not exceed 5-10% of the water depth.

The aim of this work is to evaluate the significant motions of the structure in order to proceed to fatigue analysis on the tendons [21] or on the brace system [22] due to spectral analysis.

REFERENCES

[1] C. Bak, F. Zahle, R. Bitsche, T. Kim, A. Yde, L.C. Henriksen, A. Natarajan, M.H. Hansen, "Description of the DTU 10 MW Reference Wind Turbine; DTU", in the *Wind Energy Report*-I-0092, 2013.

[2] D.N. Konispoliatis, S.A. Mavrakos, "Hydrodynamic analysis of an array of interacting free–floating oscillating water column devices," Ocean Engineering, vol. 111, pp. 179-197, 2016.

[3] D.N. Konispoliatis, T.P. Mazarakos, S.A. Mavrakos, "Hydrodynamic an analysis of three-unit arrays of floating annular oscillating-water-column wave energy converters", *Applied Ocean Research*; vol. 61, pp. 42-64, 2016.

[4] T.P. Mazarakos, D.N. Konispoliatis, T. Soukisian, S.A. Mavrakos, D. Manolas and S.G. Voutsinas, "Significant and maximum loads of a multi-purpose floating structure due to environmental conditions in the Aegean Sea," in *12th Panhellenic Symposium of Oceanography & Fisheries*, 30 May - 3 June 2018, Corfu, Greece, 2018.

[5] V. Twersky, "Multiple scattering of radiation by an arbitrary configuration of parallel cylinders," *J. Acoust. Soc. Am.* 24 (No.1) 1952.

[6] S.A. Mavrakos, P. Koumoutsakos, "Hydrodynamic interaction among vertical axisymmetric bodies restrained in waves," *Applied Ocean Research*, 9, 128-140, 1987.

[7] S.A. Mavrakos, "Hydrodynamic coefficients for groups of interacting vertical axisymmetric bodies," *Ocean Eng.* 18, 485-515, 1991.

[8] T.P. Mazarakos and S.A. Mavrakos, "Experimental investigation on mooring loads and motions of a Spar Buoy floating wind turbine," in the *Offshore Energy and Storage Symposium*, (OSES 2016), 13 - 15 July 2016, Valletta, Malta, 2016.

[9] T.P. Mazarakos, and S.A. Mavrakos, "Experimental Investigation on Mooring Loads and Motions of A TLP Floating Wind Turbine," in the *Special Session on Offshore and Marine Renewable Energy: Conversion and Transmission, Twelfth International Conference on Ecological Vehicles & Renewable Energies, EVER 2017*, Grimaldi Forum, Monaco, 2017.

[10] T.P. Mazarakos, S.A. Mavrakos, D.N. Konispoliatis, S.G. Voutsinas, D. Manolas, "Multi- purpose floating structures for offshore wind and wave energy sources exploitation," *COCONET Workshop for Offshore Wind Farms in the Mediterranean and Black Seas*, Anavyssos- Greece, 9-10 June 2014.

[11] T.P. Mazarakos, D.N. Konispoliatis, D. Manolas, S.G. Voutsinas and S.A. Mavrakos, "Modeling of an offshore multi - purpose floating structure supporting a wind turbine including second - order wave loads," in *11th European Wave and Tidal Energy Conference Series (11th EWTEC)*, 6-11 September, Nantes, France, 2015.

[12] T. P. Mazarakos, D.N. Konispoliatis and S.A. Mavrakos, "Design of a TLP floating structure concept for combined wind and wave energy exploitation," *in 2nd International Conference on Renewable Energies Offshore, (RENEW 2016)*, 24-28 October 2016, Lisbon, Portugal, 2016.

[13] T.P. Mazarakos, D.N. Konispoliatis and S.A. Mavrakos, "Geometrical Parametric Analysis of a Floating Structure of OWC Devices," in *12th International Conference on Hydrodynamics, (ICHD 2016)*, 18-23 September, Egmond aan Zee, The Netherlands, 2016.

[14] T.P. Mazarakos, D. Manolas, T. Grapsas, S.A. Mavrakos, V. Riziotis, S. Voutsinas, "Conceptual Design and advanced hydro-aero-elastic modelling of a TLP concept for Floating Wind Turbine applications," in *1st International Conference on Renewable Energies Offshore, (RENEW 2014)*, 24-26 November 2014, Lisbon, Portugal, 2014.

[15] S.A. Mavrakos, "User's Manual for the software HAMVAB," School of Naval Architecture and Marine Engineering, Laboratory for Floating Structures and Mooring Systems, 1996.

[16] ERA-20C Project (ECMWF Atmospheric Reanalysis of the 20th Century). Research Data Archive at the National Center for Atmospheric Research, Computational and Information Systems Laboratory. http://dx.doi.org/10.5065/D6VQ30QG. (Accessed 10 June 2015).

[17] S. Coles, "An Introduction to Statistical Modelling of Extreme Values," p. 209, Springer Series in Statistics, 2001.

[18] T.H. Soukissian, G. Kalantzi, "Extreme value analysis methods used for wave prediction", *Proceedings of the 16th International Offshore and Polar Engineering Conference*, Vol. III, pp. 10-17, ISBN 1-880653-66−4, 2006.

[19] Soukissian, T.H., Tsalis, C., 2015, "The effect of the generalized extreme value distribution parameter estimation methods in extreme wind speed prediction", Natural Hazards and Earth System Sciences, 78, pp. 1777–1809, Springer Netherlands.

[20] API Recommended Practice 2T, Planning, Designing, and Constructing Tension Leg Platforms, American Petroleum Institute July 2010.

[21] T. P. Mazarakos, D.N. Konispoliatis and S.A. Mavrakos, "Hydrodynamic Loading and Fatigue Analysis of an Offshore Multi - Purpose Floating Structure for Offshore Wind and Wave Energy Sources Exploitation," in *International Maritime Association of the Mediterranean, (IMAM 2017),* 9 - 13 October 2017, Lisbon, Portugal, 2017.

[22] T. P. Mazarakos, D.N. Konispoliatis and S.A. Mavrakos, "Loads On The Brace System Of An Offshore Floating Structure," in *13th International Marine Design Conference (IMDC 2018),* 11 - 14 June 2018, Helsinki, Finland, 2018.

[23] D.N. Konispoliatis, T.P. Mazarakos, T.H. Soukissian, S.A. Mavrakos, "REFOS: A multi - purpose floating platform suitable for wind and wave energy exploitation", *Proceedings, 12th International Conference on Deregulated Electricity Market Issues in South Eastern Europe (DEMSEE 2018),* September 20-21, 2018, Nicosia, Cyprus, 2018.